Copper Outdiffusion from Copper-Plated Solar Cell Contacts During Damp Heat Exposure

Joseph Karas[a#], Benjamin Phua[b], Alvin Mo[b], Nafis Iqbal[c], Kristopher Davis[c], Stuart Bowden[a], Alison Lennon[b], André Augusto[a]*

[a]Solar Power Laboratory, Arizona State University, Tempe, Arizona, 85287, United States

[b]School of Photovoltaic and Renewable Energy Engineering, University of New South Wales, Sydney, NSW, 2052, Australia

[C]Department of Materials Science and Engineering, University of Central Florida, Orlando, Florida, 32816, United States

[*]Corresponding author: joseph.f.karas@asu.edu

[#]Present address: National Renewable Energy Laboratory, Golden, Colorado, 80401, United States

Abstract

Plated copper (Cu) contacts for silicon (Si) solar cells are an attractive alternative material to conventional screenprinted silver, but there are unresolved questions on the long-term integrity of plated contact structures. In this work we perform characterization on plated Cu contacts from encapsulated cells that were degraded during extended exposure to damp heat (DH) stress. First,

using energy dispersive X-ray spectroscopy (EDS), we find evidence of Cu outdiffusion upward through capping layers made of both tin and silver applied with light-induced plating, resulting in a layer of Cu on the outer contact surface. We hypothesize that if Cu is mobile in the module, it may eventually find some route by which to enter the Si cells where it can degrade performance. Subsequently, in several types of Cu-plated, DH-degraded cells, secondary ion mass spectrometry (SIMS) detects elevated levels of Cu at the Si surface and in the Si cell bulk, which suggests that Cu can indeed migrate from contacts into Si over the course of DH stress.

Keywords: copper, tin, silver, plating, solar cell, damp heat, diffusion

I. Introduction

The long-term reliability and durability of solar cells is a topic of prime importance, particularly considering that targeted solar module lifetimes in the future may be substantially longer than the 25-30 years of field deployment that has been typical of warranties for currently-deployed modules.[1] When considering the introduction of new materials or manufacturing methods for PV modules, it should be necessary to test for and understand any new degradation modes that might also be introduced. In this case, we consider electrical contacts for silicon (Si) solar cells made primarily of plated copper (Cu), which have for some time been discussed as a lower-cost alternative to screenprinted silver (Ag) contacts.

Plated Cu contacts have not gained their projected market share for Si solar cells despite the fact that they offer savings on material costs and performance advantages compared to screenprinted Ag.[2] While there seem to be several compounding reasons for this lack of industrial adoption, a recent review of challenges with plated Cu highlighted reliability and durability concerns over

"contact integrity," a term used to describe detrimental Cu diffusion or microstructural changes in the contact over time in response to environmental stressors.[2] High-efficiency cell concepts may present an opportunity for the introduction of plated Cu contacts, as they may offer a more cost-effective route to highly-conductive contacts and are inherently formed at the low temperatures necessitated by some high-efficiency cell passivation schemes.[3,4] Therefore, continued study of plated Cu contact integrity is important.

Copper ingress from contacts into Si has been a concern from the outset as Cu is a particularly fast-diffusing and insidious defect in Si and can form highly recombination-active precipitates.[5–7] Plated contact schemes aim to prevent Cu ingress with diffusion barriers between the Cu and Si. In homojunction c-Si cells with direct contact between metal and Si, this barrier layer is usually nickel (Ni), and is usually annealed to form an interfacial nickel silicide layer ($NiSi_X$). The annealed Ni layer is also understood to improve adhesion and reduce contact resistance.[8–12] A number of studies have tested for the downward diffusion of Cu (into cells) through the Ni barrier by means of accelerated testing at elevated temperatures (usually 200°C), with detrimental degradation noted only when the Ni layer is insufficiently thick (<~200 nm).[13,14] It is assumed that with sufficiently thick Ni barriers, the downward ingress of Cu is prevented both by the formation of $NiSi_X$ layer at the bottom of the stack and alloying at the Ni-Cu interface.[2,15,16] However, one study showed detrimental Cu precipitates underneath Ni diffusion barriers after 200°C heat treatments and rapid cooling, suggesting that downward Cu may somehow defeat Ni barriers at moderate temperatures, but that slow cooling inhibits the formation of performance-limiting extended Cu defects.[17]

More recently, other evidence has emerged regarding another aspect of contact integrity: after performing extended heat treatments designed to test for downward Cu diffusion, several studies

have found evidence of "upward" Cu outdiffusion through Ag capping layers, which can leave voids in the contact stack that in some cases ultimately affected device performance.[10,18,19]

In previous work, we have shown that encapsulated cells with Cu-plated contacts degrade more under damp heat (DH) stress than comparative encapsulated cells with Ag-screenprinted contacts.[20,21] Specifically, the degradation in Cu-plated samples affected diode parameters, indicating junction degradation described by increasing non-ideal recombination current density (J_{02}) and decreasing pseudo fill factor (pFF) as measured by the Suns-V_{OC} technique.[22] In the first study, the degradation was not observed in sister samples with Ag-screenprinted contacts, and degradation was prevented in Cu-plated cells when the encapsulant was polyolefin elastomer (POE), rather than the more common ethylene vinyl acetate (EVA).[20] In the second study, degradation seemed to correlate with the average adhesion strength of the Cu-plated fingers to Si, and it was proposed that weaker finger adhesion resulted in finger dislodgement during DH testing, thereby opening a pathway for mobile Cu to diffuse into Si.[21]

In the present work we examine samples from those previous studies that exhibited pFF loss after DH stress. We hypothesized that this degradation could be due to Cu contamination of the Si. We present cross-sectional scanning electron microscope (SEM) images and energy dispersive X-ray spectroscopy (EDS) characterization of encapsulated, Cu-plated cells after exposure to 1000+ hours of DH testing at 85°C and 85% relative humidity. In these modules, we find evidence of Cu diffusion outward through contact capping layers formed by light-induced plating (LIP). In samples with suspected Cu-induced degradation, we show evidence of Cu ingress into c-Si via secondary ion mass spectroscopy (SIMS).

II. Experimental

The samples in this work are a variety of p-type c-Si cells with Ni-Cu plated contacts, which were encapsulated into modules, and exposed to DH at 85°C and 85% relative humidity (RH) for varying durations. As described in subsequent sections, we examined several different cells with plated Cu contacts manufactured with different specific processes and encapsulated with different materials. In particular, we study Ni-Cu plated contacts with different metal capping layers: both tin (Sn) applied with light-induced plating (LIP Sn) and silver (Ag), also applied with LIP (LIP Ag). Although the specific materials, manufacturing, DH stress duration and observed degradation in each sample are slightly different, we aim to compare and contrast Cu outdiffusion in different systems. More details of each sample are found in respective discussion in Sections III.A and III.B.

After DH exposure, samples were characterized with I-V and electroluminescence and/or photoluminescence imaging, then prepared for cross-sectional imaging. Small, selected sections of modules were removed with a diamond cutter, then mounted in resin for grinding and polishing. Glass and encapsulant were ground away, then polished with 3 μm and 1 μm compound until smooth. A Helios G4 plasma focused ion beam and scanning electron microscope (PFIB-SEM) was used to mill EVA and plated finger cross sections and take images, equipped with an Oxford Ultim Max 170 SDD energy dispersive X-ray spectroscopy (EDS) system for elemental mapping.

Selected sections of the same and analogous modules were analyzed with secondary ion mass spectroscopy (SIMS). After harvesting cores from degraded modules and removing the encapsulant, the samples were dipped in 70% nitric acid (HNO_3) for 90 minutes at 45°C followed by 5% hydrofluoric acid (HF) for 4 minutes to remove the metallization and expose the silicon surface. SIMS was performed using a PHI Adept 1010 Dynamic SIMS system, with an oxygen primary ion beam with 3 kV energy and 20 nA current. The raster size was 60 x 60 μm and positive ions were detected from a 19 x 19 μm area in the center. Multiple measurements were performed

at exposed metal contact regions on each sample. See the discussion of SIMS measurements applied to degraded c-Si cells in Iqbal et al.[23]

III. Results and Discussion

III. A. Electron microscopy and EDS of degraded samples

III. A. 1. Cu-plated, Sn-capped

Electroluminescence (EL) images of a degraded Cu-plated Sn-capped cell over 2000 hours of DH are shown in Figure 1. The pFF of the sample decreased from 82.1% to 77.0% and J_{02} more than doubled, indicating degradation of the diode characteristics of the cell.[22]

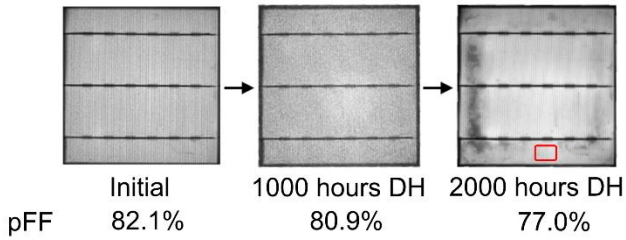

Figure 1. Electroluminescence and pFF changes of a Cu-plated, Sn-capped cell over 2000 hours of DH exposure. The area harvested for SEM cross-sectioning is indicated in red.

Figure 2a shows a SEM cross section of a Ni-Cu-Sn-plated contact finger harvested from the cell region indicated in Figure 1. This cell was fabricated from a 6" textured p-type mono-Si aluminum back surface field (Al-BSF) cell precursor obtained from an industrial manufacturer, lacking a front contact. The front contact pattern was then patterned via negative screenprinted photoresist, and the Si surface was exposed for plating via HF etching of the front silicon nitride antireflection coating. The aspect ratio of the contacts was rather large due to the poor fidelity of resist/wet etch patterning: fingers were roughly 200 μm wide by several μm tall. The plated contact

stack was formed via light-induced plating (LIP): first a Ni diffusion barrier from a sulfamate-based Ni bath. Following a $NiSi_X$-forming anneal (350°C, 2 minutes, N_2 ambient) and SPM etch (2 minutes, 4:1 sulfuric acid to hydrogen peroxide) of unreacted Ni, the final stack was plated with LIP Ni, sulfate-based LIP Cu, and LIP acid stannous Sn with interim rinsing.[24] The final contact stack height at the busbar was approximately 7-8 μm, roughly 0.5 μm Ni, 6 μm Cu, and 1 μm Sn. The sample was tabbed by hand and encapsulated with a conventional glass/EVA/backsheet module construction and subjected to 2000 total hours of 85°C/85% RH DH stress.

Figure 2c shows linescan EDS data from the yellow line indicated in 2a. Figure 2b shows EDS maps, which clearly show the presence of Cu within the Sn capping layer, and particularly accumulating at the outer Sn surface. Small voids are visible at the Cu-Sn interface approximately every 1-2 μm.

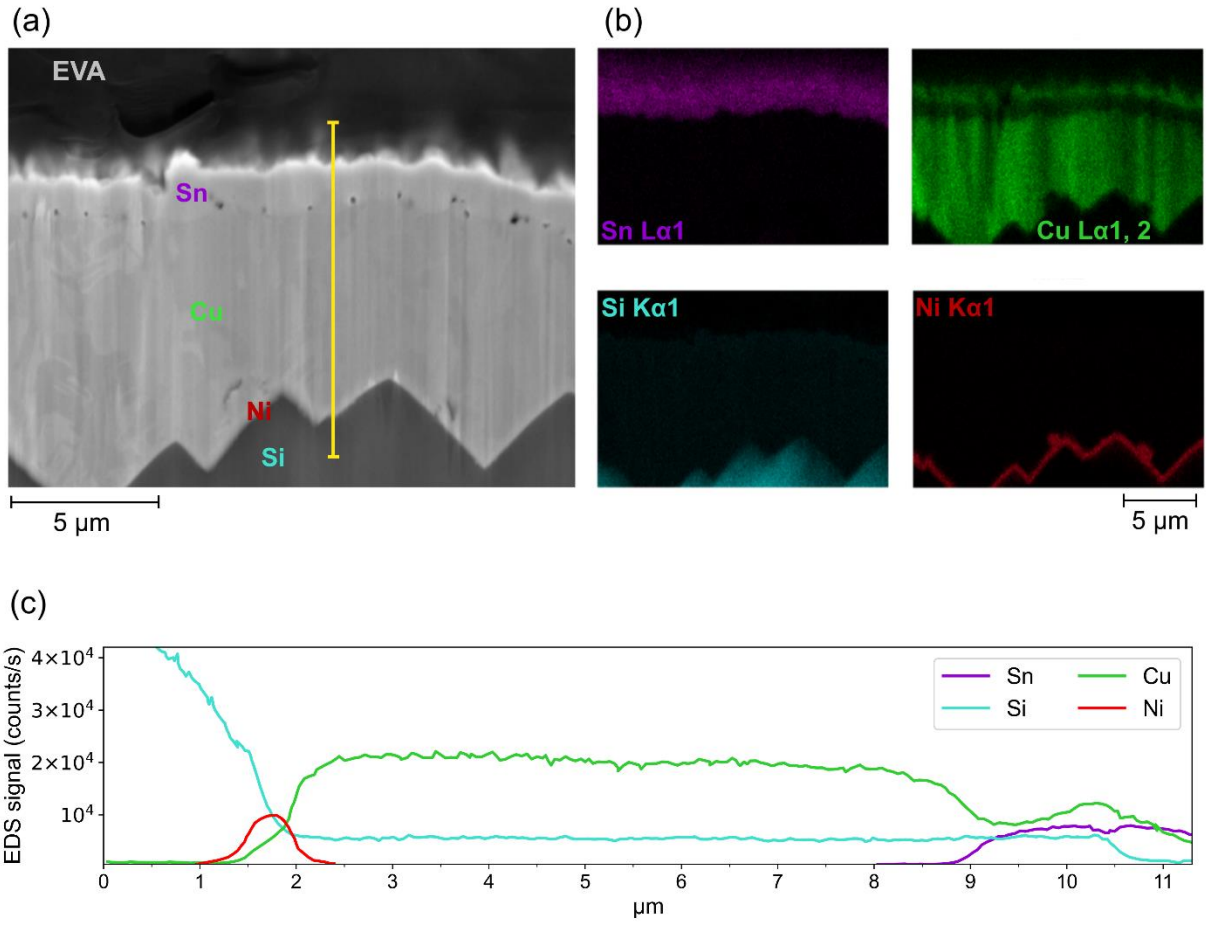

Figure 2. (a) SEM cross section of a Ni-Cu-Sn plated contact finger harvested from the region indicated in Figure 1 after 2000 hours of DH. **(b)** EDS maps for Sn, Cu, Ni, and Si of the same cross section. **(c)** EDS linescan of the line indicated in (a).

The low temperature Cu-Sn system has been studied extensively, primarily regarding solid state Cu-Sn interdiffusion which results in intermetallic compounds (IMCs). These IMCs are problematic in solder joints because of their brittleness.[25] Cu is a fast diffuser in Sn, diffusing interstitially in the *c* direction of the metallic Sn tetragonal lattice, which initiates Cu-Sn interdiffusion at low temperature.[26] The Cu-Sn phase diagram shows two low-temperature IMCs formed through interdiffusion: an orthorhombic ε-Cu_3Sn and a monoclinic η-Cu_6Sn_5.[27,28] Many

experimental results on binary Cu-Sn diffusion couples at low temperatures find that these two phases develop at Cu-Sn interfaces.[29] A number of measured and derived Cu-Sn interdiffusion concentration profiles from the literature appear much the same as the EDS profile near the Cu-Sn interface in Figure 2c, see for example Kumar et al.[30]

Another feature of many of these studies of Cu-Sn interdiffusion is the development of microvoids at the interface, which are attributed to the faster diffusion of Cu into Sn than Sn into Cu, as well as in the IMC layers.[30,31] This results in a net flux of vacancies, which can coalesce to form voids. While these are frequently called "Kirkendall voids" in the literature, the position of the voids in the IMC layers requires some extension of classical Kirkendall theory. In particular, multiple Kirkendall planes are predicted in the Cu-Sn system, an effect of the diffusion anisotropy of the Cu-Sn IMCs.[29,32] Furthermore, it has been shown repeatedly that void formation is enhanced by the presence of impurities, which is very relevant for plated Cu from sulfate-based acid solutions, which is likely to have impurities including sulfur, chlorine, carbon, and oxygen.[31,33,34] Void size and density in plated Cu-Sn also seems to depend on plating current density.[35] In the Cu-Sn system, voids are expected to form at the Cu-Cu_3Sn interface, and perhaps within the Cu_3Sn phase, especially if the purity of the Cu layer is ≤99.9%.[30] While Cu diffusion in Sn is a predominantly bulk diffusion process, grain boundary diffusion plays an important role in transporting Sn in the Cu_6Sn_5 layer toward the Cu_3Sn layer, so the Cu_6Sn_5 tends to consume the Cu_3Sn.[36] Grain boundary diffusion explains why Sn and Cu diffusion in the Cu_6Sn_5 phase are roughly equal. If left for long periods, the growth of voids in the Cu_3Sn layer may disrupt the diffusion of Cu, and eventually the Cu_3Sn is consumed by Cu_6Sn_5.[35] At low temperatures (<75°C) it seems like the primary phase growth is in the Cu_6Sn_5 phase, whereas at higher temperatures both phases grow.[37] This difference in phase growth is potentially relevant for Cu-plated solar cell

contacts in the field, which operate in wide temperature ranges that will typically be lower than 75°C, but may occasionally approach 75°C in hot climates. It may also suggest that the phase growth will be different in most field scenarios than in 85°C DH testing.

Overall, the implication seems to be that some degree of IMC and void growth should be anticipated with plated Cu-Sn contacts. With a sufficiently thick Sn layer, growth of the Cu_6Sn_5 phase could ultimately present a barrier to further outdiffusion of Cu through Sn. Cu outdiffusion will also be disrupted as voids form at the Cu-Cu_3Sn interface.[35] Both are dependent on temperature and Cu purity, among other variables. With a thin layer of Sn and/or no limitation on Cu outdiffusion, Cu-Sn IMCs could potentially consume the entire Sn layer given enough time. Another solution might be to add Ni to the Cu (5-15 at.%, or 9 at.% according to various sources), to limit Cu outdiffusion and create a stable phase of $(Cu, Ni)_6Sn_5$ at room temperature.[27,38]

III. A. 2. Cu-plated, Ag-capped

Figure 3 shows cross-sectional and luminescence data from a 3x3 cm cell with Ni-Cu-Ag plated contacts. This cell was fabricated from a 156 x 156 mm PERC precursor without front contacts. Twenty-five small cell contact grids (25 x 25 mm) were patterned on the front of each wafer by removal of the silicon nitride antireflection layer with a 266 nm ps Lumera Super Rapid Nd: YAG laser with a BBO crystal for the 4th harmonic. Pre-treatment (deglazing) was performed by single side immersion in 1% HF for 60 s to remove native oxides formed during laser ablation followed by a rinse with deionized water.[39,40] LIP was used for the Ni (~1 μm), Cu (~11 μm) and Ag (~1 μm) contact stack. After cells were plated, they were annealed (350°C, 1 minute, N_2 ambient) to form $NiSi_x$. After annealing, each large precursor was laser cleaved into 25 individual small cells (30 x 30 mm).[40] Cells were interconnected and EVA-encapsulated in a three-cell mini-module and

exposed to 1000 hours of DH stress. pFF reduced from 79.4% to 77.9% in DH, again indicating deterioration of the diode characteristics.

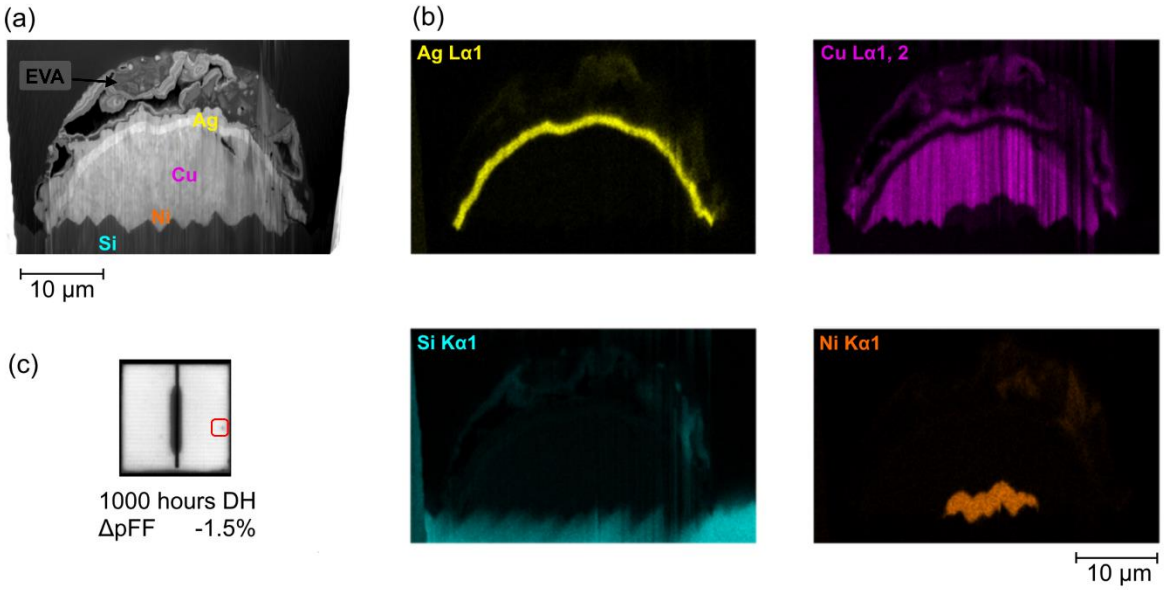

Figure 3. **(a)** SEM cross section of a finger from a Ni-Cu-Ag plated cell after 1000 hours of DH, harvested from the region indicated in (c). **(b)** EDS maps of the same cross section for Ag, Cu, Si, and Ni. **(c)** EL and pFF loss for the cell after 1000 hours of DH.

Figure 3a shows the cross-sectional image of a finger, harvested from the region indicated in Figure 3c. The EDS map of the cross section in Figure 3b shows the presence of the Cu on the outer surface of the capping layer and interestingly lining the voids in the encapsulant above the finger. Close inspection shows small voids present at the Cu-Ag interface. Previously, small voids have been reported at the interface of LIP Cu and LIP Ag after $NiSi_x$ annealing at 300-350°C for several minutes,[21,41] with larger voids reported after thermally-stressing cells at 200°C for 500 hours.[10,42]

The Cu-Ag phase diagram predicts little solid solubility in the Cu-Ag system below the eutectic point at approximately 780°C, therefore bulk diffusion studies seldom report interdiffusion in Cu-

Ag diffusion couples below ~700°C.[43–46] In other cases, diffusion experiments at lower temperature have noted a discontinuity in the Arrhenius plot of Cu-Ag diffusion coefficient, indicating a lower activation energy at temperatures below 600-700°C, which they attribute to the greater role played by grain boundary diffusion.[47,48] Dorner et al. took care to study Cu diffusion in Ag single crystals and found no such discontinuity in the Arrhenius plot, again suggesting that grain boundary diffusion is responsible for diffusion of Cu in Ag at temperatures below the limit of solid solubility.[49]

Applied studies of Cu diffusion through thin plated Ag layers have been previously performed on leadframe packages for integrated circuits. Lin et al. detected Cu migration through 5-7 μm-thick plated Ag layers after 2.5 hours at 175°C, and suggested that grain boundaries in the Ag layer presented a route for Cu migration.[50] Similar experiments were performed by Li and Ong and Zhang et al.,[51,52] who all discovered Cu migration through several μm of plated Ag after thermal exposure to 125-200°C for durations ranging from several hours to several days. A point of emphasis in these studies was the consumption of outdiffused Cu by reactions occurring on the surface. Cu oxidized with atmospheric oxygen or corroded from oxygen and sulfur present in packaging mold compounds. The rate of Cu outdiffusion through Ag seemed to depend on the chemical environment at the outer surface of the Ag layer, with some packages preventing Cu outdiffusion better than others.[50–52] Similarly, chemically-driven outdiffusion of Cu through plated Ag grain boundaries is observed in historical daguerreotype photographs.[53,54]

Therefore, it seems plausible that Cu could outdiffuse through plated Ag capping layers at relatively low temperature, given both sufficient grain boundaries in the Ag layer and a chemical reaction "sink" at the surface. It is well known that DH stress applied to conventional PV modules with EVA encapsulant produces acetic acid. Acetic acid has been noted to corrode cell

metallization in other experiments (see e.g. references [55,56]); in Cu-plated, Ag-capped samples it might also provide a sink reaction to drive Cu outdiffusion via grain boundaries. Solutions to prevent this outdiffusion may be to substitute or engineer encapsulant materials to produce less acetic acid; or to manipulate the grain boundaries of the Ag layer to provide fewer diffusion pathways. Colwell et al. noted apparently greater Cu outdiffusion through thick LIP Ag capping layers than in thin immersion-plated Ag, and suggested the more polycrystalline LIP Ag provided more pathways for low-temperature Cu diffusion.[18]

III. B. SIMS on degraded samples

After finding evidence of Cu outdiffusion, it is important to understand if the outdiffused Cu is problematic. In an effort to understand if degradation of diode characteristics is actually caused by Cu ingress into the c-Si, SIMS profiles into the depth of the c-Si were recorded on a number of locations on a number of different sample types. Figure 4 shows SIMS depth profiles of Cu in three samples with different DH degradation. The signal is normalized to the maximum detected signal. Lines represent the mean of multiple measurements from a sample, shaded areas represent the 95% confidence interval. Ni-Cu-Sn plated (EVA) (solid black line) signifies a sample analogous to the one discussed in Section III.A.1 and Figures 1 and 2: that is, a cell with Cu-plated, LIP Sn-capped contacts, encapsulated in EVA. It was exposed to 3500 hours of 85°C/85% RH DH and lost 4.7% absolute of pFF with more than 6x increase in J_{02}. Ni-Cu-Sn plated (POE) (dashed red line) is the same type of sample except encapsulated in POE, and did not undergo appreciable pFF or J_{02} degradation over the same duration of DH. The EVA sample has a roughly three-fold greater concentration of Cu at the surface than the POE sample, on average. The rather large

confidence interval could reflect the fact that these dynamic SIMS depth profiles are complicated by the Si surface texture. We also cannot rule out that Cu ingress could vary across the surface of each sample, which would also yield large confidence intervals. As a reference, Figure 4 also shows a profile (dotted blue line) from a Ag screenprinted sister cell, encapsulated in EVA, which did not degrade over 3500 hours of DH, and shows essentially no Cu signal. The surface concentration of Cu shown in Figure 4 is higher in the Cu-plated, EVA-encapsulated sample than in the Cu-plated, POE-encapsulated sample. We have previously reported that the diode degradation was greater in EVA-encapsulated samples than in POE-encapsulated samples[20], and we now suggest the reason is because Cu ingress is greater EVA-encapsulated samples.

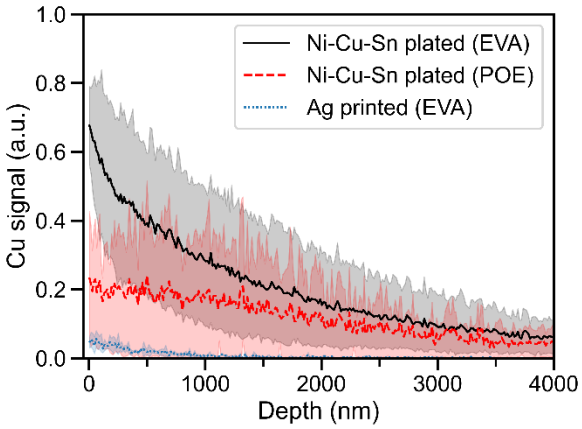

Figure 4. SIMS Cu profiles into three similar c-Si solar cells after 3500 hours of DH: a Ni-Cu-Sn plated cell, encapsulated in EVA (solid black line); a Ni-Cu-Sn plated cell encapsulated in POE (dashed red line); and a Ag-screenprinted cell encapsulated in EVA (dotted blue line). The line shows the mean of multiple measurements (five, three, and two measurements respectively) and the shaded area shows the 95% confidence interval.

Figure 5 shows SIMS profiles from a Cu-plated, LIP Ag-capped sample with a contact stack similar to the one discussed in Section III.A.2 and Figure 3. It was encapsulated in EVA, and

exposed to 2000 hours of DH and degraded in pFF 6.8% absolute. The bad regions (orange solid line) are measurements performed on areas that appeared relatively darker in EL, while the good regions (green dashed line) are measurements performed on bright areas, marked in the EL image. We detect Cu in the sample in both good and bad areas. The surface concentration of Cu is greater in the bad regions, but the good regions have slightly higher Cu signal beyond ~500 nm. This might indicate that Cu is more concentrated in the emitter in worse-performing regions.

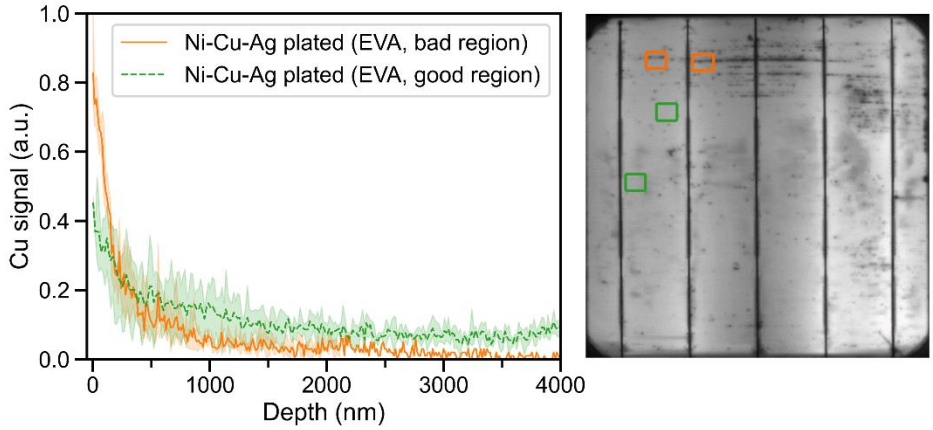

Figure 5. SIMS Cu profiles into a Ni-Cu-Ag plated cell, encapsulated in EVA, after 2000 hours of DH. Bad regions (solid orange line) correspond to dark spots in EL indicated in the image at right. Good regions (dashed green line) correspond to brighter areas. The line shows the mean of 3 measurements from each region, the shaded area shows the 95% confidence interval.

V. Conclusion

This study of DH-exposed silicon solar cells with Cu-plated contacts shows evidence of Cu outdiffusion through plated capping layers after 1000+ hours of DH exposure. Outdiffusion is

observed for both LIP Sn and LIP Ag capping, although in each case the mechanism for low temperature outdiffusion is likely different. In Cu-Sn contacts, low temperature formation of IMC layers via interdiffusion at the interface is predicted by the Cu-Sn phase diagram. In Cu-Ag contacts, Cu outdiffusion is likely confined to grain boundaries, and perhaps only if a chemical driving force consumes outdiffused Cu at the surface.

Cells with both Cu-Sn and Cu-Ag contact stacks exhibited pFF loss in DH. Previous studies of Cu contact-induced degradation have primarily been concerned with pFF loss caused by downward Cu ingress through seed/barrier layers (usually Ni). Upward Cu outdiffusion may also need to be considered, particularly in module packages that create a chemical reaction sink at the outer surface of the contact, e.g., acetic acid from hydrolyzed EVA. Once outdiffused, Cu may be mobile in the module and eventually find some route to ingress into the Si. Conceivable solutions are to engineer the capping layers to prevent Cu outdiffusion, or to remove the driving force for outdiffusion by better engineering module packages and materials for stable chemical environments, for example, by replacing EVA with other encapsulants.

Finally, we present evidence of Cu ingress into c-Si in several types of Cu-plated, DH-degraded cells as measured by SIMS. In general, the relative quantity of Cu measured by SIMS at the c-Si surface correlates with the extent of degradation observed in I-V parameters or observed in electroluminescence. We have shown evidence that replacing EVA with POE seems to limit Cu ingress.

Acknowledgements

This work was supported in part by the U.S. Department of Energy's Office of Energy Efficiency and Renewable Energy (DOE EERE) Solar Energy Technologies Office (SETO) under SolarMat

2 Award Number DE-EE0006814, Award Number DE-EE0008155, and Agreement 32509 for the Durable Module Materials Consortium (DuraMAT), and in part by the Engineering Research Center Program of the National Science Foundation (NSF) and the DOE EERE under NSF Cooperative Agreement EEC-1041895 (QESST). Additionally, this work has been supported in part by the Australian Research Council Future Fellowship FT170100447 (Alison Lennon) and the Australian Government through a Research Training Scholarship awarded to Ben Phua. The authors gratefully thank L. Michaelson, K. Munoz, and T. Tyson of Technic, Inc. for sample preparation and support of this work.

Conflicts of Interest: The authors declare no conflicts of interest.

References

(1) Wilson, G. M.; Al-Jassim, M.; Metzger, W. K.; Glunz, S. W.; Verlinden, P.; Xiong, G.; Mansfield, L. M.; Stanbery, B. J.; Zhu, K.; Yan, Y.; Berry, J. J.; Ptak, A. J.; Dimroth, F.; Kayes, B. M.; Tamboli, A. C.; Peibst, R.; Catchpole, K.; Reese, M. O.; Klinga, C. S.; Denholm, P.; Morjaria, M.; Deceglie, M. G.; Freeman, J. M.; Mikofski, M. A.; Jordan, D. C.; TamizhMani, G.; Sulas-Kern, D. B. The 2020 Photovoltaic Technologies Roadmap. *J. Phys. D. Appl. Phys.* **2020**, *53* (49), 493001. https://doi.org/10.1088/1361-6463/ab9c6a.

(2) Lennon, A.; Colwell, J.; Rodbell, K. P. Challenges Facing Copper-Plated Metallisation for Silicon Photovoltaics: Insights from Integrated Circuit Technology Development. *Prog. Photovoltaics Res. Appl.* **2019**, *27* (1), 67–97. https://doi.org/10.1002/pip.3062.

(3) Grübel, B.; Cimiotti, G.; Arya, V.; Fellmeth, T.; Feldmann, F.; Steinhauser, B.; Kluska, S.; Kluge, T.; Landgraf, D.; Glatthaar, M. Plated Ni/Cu/Ag for TOPCon Solar Cell Metallization. In *36th European Photovoltaic Solar Energy Conference and Exhibition*; Marseille, 2019; pp 167–171. https://doi.org/10.4229/EUPVSEC20192019-2BO.2.3.

(4) Hatt, T.; Bartsch, J.; Davis, V.; Richter, A.; Kluska, S.; Glunz, S. W.; Glatthaar, M.; Fischer, A. Hydrophobic AlOx Surfaces by Adsorption of a SAM on Large Areas for Application in Solar Cell Metallization Patterning. *ACS Appl. Mater. Interfaces* **2021**, *13* (4), 5803–5813. https://doi.org/10.1021/acsami.0c20134.

(5) Istratov, A. A.; Flink, C.; Hieslmair, H.; Weber, E. R.; Heiser, T. Intrinsic Diffusion Coefficient of Interstitial Copper in Silicon. *Phys. Rev. Lett.* **1998**, *81* (6), 1243–1246. https://doi.org/10.1103/PhysRevLett.81.1243.

(6) Istratov, A. A.; Hedemann, H.; Seibt, M.; Vyvenko, O. F.; Schroter, W.; Heiser, T.; Flink,

C.; Hieslmair, H. H.; Weber, E. Electrical and Recombination Properties of Copper-Silicide Precipitates in Silicon. *J. Electrochem. Soc.* **1998**, *145* (11), 3889. https://doi.org/10.1149/1.1838889.

(7) Istratov, A. A.; Weber, E. R. Physics of Copper in Silicon. *J. Electrochem. Soc.* **2002**, *149* (1), G21. https://doi.org/10.1149/1.1421348.

(8) ur Rehman, A.; Lee, S. H.; Bhopal, M. F.; Lee, S. H. Ni/Cu/Ag Plated Contacts: A Study of Resistivity and Contact Adhesion for Crystalline-Si Solar Cells. *Electron. Mater. Lett.* **2016**, *12* (4), 439–444. https://doi.org/10.1007/s13391-016-4003-2.

(9) Bajpai, V. K.; Pant, P.; Solanki, C. S. Thin Uniform Nickel Seed Layer Formation and Its Impact on Ni-Cu Contact Adhesion for c-Si Solar Cell Applications. *Sol. Energy* **2017**, *155*, 62–74. https://doi.org/10.1016/j.solener.2017.06.002.

(10) Dang, C.; Labie, R.; Simoen, E.; Poortmans, J. Detailed Structural and Electrical Characterization of Plated Crystalline Silicon Solar Cells. *Sol. Energy Mater. Sol. Cells* **2018**, *184*, 57–66. https://doi.org/10.1016/j.solmat.2018.04.016.

(11) Buchler, A.; Grubel, B.; Arya, V.; Weingartner, T.; Hahnel, A.; Naumann, V.; Bartsch, J.; Glatthaar, M.; Kluska, S. Microcharacterization of Interface Oxide Layer on Laser-Structured Silicon Surfaces of Plated Ni–Cu Solar Cells. *IEEE J. Photovoltaics* **2019**, *9* (6), 1532–1540. https://doi.org/10.1109/JPHOTOV.2019.2938306.

(12) Aleem, M.; Vishnuraj, R.; Krishnan, B.; Pullithadathil, B. Realization of Micropatterned, Narrow Line-Width Ni–Cu–Sn Front Contact Grid Pattern Using Maskless Direct-Write Lithography for Industrial Silicon Solar Cells. *ACS Appl. Energy Mater.* **2021**, *4* (10), 10682–10696. https://doi.org/10.1021/acsaem.1c01699.

(13) Bartsch, J.; Mondon, A.; Bayer, K.; Schetter, C.; Hörteis, M.; Glunz, S. W. Quick Determination of Copper-Metallization Long-Term Impact on Silicon Solar Cells. *J. Electrochem. Soc.* **2010**, *157* (10), H942. https://doi.org/10.1149/1.3466984.

(14) Kraft, A.; Wolf, C.; Bartsch, J.; Glatthaar, M.; Glunz, S. Long Term Stability of Copper Front Side Contacts for Crystalline Silicon Solar Cells. *Sol. Energy Mater. Sol. Cells* **2015**, *136*, 25–31. https://doi.org/10.1016/j.solmat.2014.12.024.

(15) Nicolet, M.; Bartur, M. Diffusion Barriers in Layered Contact Structures. *J. Vac. Sci. Technol.* **1981**, *19* (3), 786–793. https://doi.org/10.1116/1.571149.

(16) Kale, A. S.; Nemeth, W.; Perkins, C. L.; Young, D.; Marshall, A.; Florent, K.; Kurinec, S. K.; Stradins, P.; Agarwal, S. Thermal Stability of Copper–Nickel and Copper–Nickel Silicide Contacts for Crystalline Silicon. *ACS Appl. Energy Mater.* **2018**, *1* (6), 2841–2848. https://doi.org/10.1021/acsaem.8b00488.

(17) Flynn, S.; Lennon, A. Copper Penetration in Laser-Doped Selective-Emitter Silicon Solar Cells with Plated Nickel Barrier Layers. *Sol. Energy Mater. Sol. Cells* **2014**, *130*, 309–316. https://doi.org/10.1016/j.solmat.2014.07.026.

(18) Colwell, J.; Hsiao, P.-C.; Shen, X.; Zhang, W.; Wang, X.; Lim, S.; Lennon, A. Impact of Contact Integrity during Thermal Stress Testing on Degradation Analysis of Copper-Plated Silicon Solar Cells. *Sol. Energy Mater. Sol. Cells* **2018**, *174*, 225–232.

https://doi.org/10.1016/j.solmat.2017.09.005.

(19) Lee, S. H.; Lee, D. W.; Rehman, A. U.; Baik, J. W.; Lee, S. H. Study of Annealing Temperature for Ni/Cu/Ag Plated Front Contact Single Crystalline Solar Cells. *IEEE J. Photovoltaics* **2016**, *6* (5), 1090–1093. https://doi.org/10.1109/JPHOTOV.2016.2576683.

(20) Karas, J.; Michaelson, L.; Munoz, K.; Jobayer Hossain, M.; Schneller, E.; Davis, K. O.; Bowden, S.; Augusto, A. Degradation of Copper-plated Silicon Solar Cells with Damp Heat Stress. *Prog. Photovoltaics Res. Appl.* **2020**, *28* (11), 1175–1186. https://doi.org/10.1002/pip.3331.

(21) Phua, B.; Shen, X.; Hsiao, P.; Kong, C.; Stokes, A.; Lennon, A. Degradation of Plated Silicon Solar Module Due to Copper Diffusion: The Role of Capping Layer Formation and Contact Adhesion. *Sol. Energy Mater. Sol. Cells* **2020**, *215*, 110638. https://doi.org/10.1016/j.solmat.2020.110638.

(22) Sinton, R. A.; Cuevas, A. A Quasi-Steady-State Open-Circuit Voltage Method for Solar Cell Characterization. In *16th European Photovoltaic Solar Energy Conference*; 2000; Vol. 25, pp 1152–1155.

(23) Iqbal, N.; Colvin, D. J.; Curran, A. J.; Li, F.; Ganesan, J. P.; Sulas-Kern, D. B.; Harvey, S.; Norman, A.; Karas, J.; TamizhMani, G.; Jaubert, J.-N.; Banerjee, P.; Huey, B. D.; French, R. H.; Davis, K. O. Multiscale Characterization of Photovoltaic Modules—Case Studies of Contact and Interconnect Degradation. *IEEE J. Photovoltaics* **2022**, *12* (1), 62–72. https://doi.org/10.1109/JPHOTOV.2021.3124751.

(24) Michaelson, L. M.; Munoz, K.; Karas, J.; Bowden, S.; Rand, J. A.; Gallegos, A.; Tyson, T.; Buonassisi, T. *Silver-Free Metallization Technology for Producing High Efficiency, Industrial Silicon Solar Cells*; DOE-TECHNIC-6814; Golden, CO (United States), 2018. https://doi.org/10.2172/1432485.

(25) Frear, D. R.; Vianco, P. T. Intermetallic Growth and Mechanical Behavior of Low and High Melting Temperature Solder Alloys. *Metall. Mater. Trans. A* **1994**, *25* (7), 1509–1523. https://doi.org/10.1007/BF02665483.

(26) Dyson, B. F.; Anthony, T. R.; Turnbull, D. Interstitial Diffusion of Copper in Tin. *J. Appl. Phys.* **1967**, *38* (8), 3408–3408. https://doi.org/10.1063/1.1710127.

(27) Paul, A. The Kirkendall Effect in Solid State Diffusion, Eindhoven University of Technology, 2004.

(28) Fürtauer, S.; Li, D.; Cupid, D.; Flandorfer, H. The Cu–Sn Phase Diagram, Part I: New Experimental Results. *Intermetallics* **2013**, *34*, 142–147. https://doi.org/10.1016/j.intermet.2012.10.004.

(29) Paul, A.; Ghosh, C.; Boettinger, W. J. Diffusion Parameters and Growth Mechanism of Phases in the Cu-Sn System. *Metall. Mater. Trans. A* **2011**, *42* (4), 952–963. https://doi.org/10.1007/s11661-010-0592-9.

(30) Kumar, S.; Handwerker, C. A.; Dayananda, M. A. Intrinsic and Interdiffusion in Cu-Sn System. *J. Phase Equilibria Diffus.* **2011**, *32* (4), 309–319. https://doi.org/10.1007/s11669-011-9907-9.

(31) Baheti, V. A.; Kashyap, S.; Kumar, P.; Chattopadhyay, K.; Paul, A. Bifurcation of the Kirkendall Marker Plane and the Role of Ni and Other Impurities on the Growth of Kirkendall Voids in the Cu–Sn System. *Acta Mater.* **2017**, *131*, 260–270. https://doi.org/10.1016/j.actamat.2017.03.068.

(32) Paul, A.; van Dal, M. J. H.; Kodentsov, A. A.; van Loo, F. J. J. The Kirkendall Effect in Multiphase Diffusion. *Acta Mater.* **2004**, *52* (3), 623–630. https://doi.org/10.1016/j.actamat.2003.10.007.

(33) Jung, Y.; Yu, J. Electromigration Induced Kirkendall Void Growth in Sn-3.5Ag/Cu Solder Joints. *J. Appl. Phys.* **2014**, *115* (8), 083708. https://doi.org/10.1063/1.4867115.

(34) Liu, C.-W.; Wang, Y.-L.; Tsai, M.-S.; Feng, H.-P.; Chang, S.-C.; Hwang, G.-J. Effect of Plating Current Density and Annealing on Impurities in Electroplated Cu Film. *J. Vac. Sci. Technol. A Vacuum, Surfaces, Film.* **2005**, *23* (4), 658–662. https://doi.org/10.1116/1.1931679.

(35) Ross, G.; Vuorinen, V.; Paulasto-Kröckel, M. Void Formation and Its Impact on Cu Sn Intermetallic Compound Formation. *J. Alloys Compd.* **2016**, *677*, 127–138. https://doi.org/10.1016/j.jallcom.2016.03.193.

(36) Svoboda, J.; Fischer, F. D.; Schillinger, W. Formation of Multiple Stoichiometric Phases in Binary Systems by Combined Bulk and Grain Boundary Diffusion: Experiments and Model. *Acta Mater.* **2013**, *61* (1), 32–39. https://doi.org/10.1016/j.actamat.2012.09.008.

(37) Baheti, V. A.; Kashyap, S.; Kumar, P.; Chattopadhyay, K.; Paul, A. Solid–State Diffusion–Controlled Growth of the Intermediate Phases from Room Temperature to an Elevated Temperature in the Cu–Sn and the Ni–Sn Systems. *J. Alloys Compd.* **2017**, *727*, 832–840. https://doi.org/10.1016/j.jallcom.2017.08.178.

(38) Nogita, K.; Nishimura, T. Nickel-Stabilized Hexagonal (Cu,Ni)6Sn5 in Sn–Cu–Ni Lead-Free Solder Alloys. *Scr. Mater.* **2008**, *59* (2), 191–194. https://doi.org/10.1016/j.scriptamat.2008.03.002.

(39) Hsiao, P.-C.; Song, N.; Wang, X.; Shen, X.; Phua, B.; Colwell, J.; Romer, U.; Johnston, B.; Lim, S.; Shengzhao, Y.; Verlinden, P.; Lennon, A. 266-Nm Ps Laser Ablation for Copper-Plated p-Type Selective Emitter PERC Silicon Solar Cells. *IEEE J. Photovoltaics* **2018**, *8* (4), 952–959. https://doi.org/10.1109/JPHOTOV.2018.2834629.

(40) Shen, X.; Hsiao, P.; Phua, B.; Stokes, A.; Gonçales, V. R.; Lennon, A. Plated Metal Adhesion to Picosecond Laser-Ablated Silicon Solar Cells: Influence of Surface Chemistry and Wettability. *Sol. Energy Mater. Sol. Cells* **2020**, *205*, 110285. https://doi.org/10.1016/j.solmat.2019.110285.

(41) Lee, S. H.; Lee, D. W.; Rehman, A. ur; Baik, J. W.; Lee, S. H. Study of Annealing Temperature for Ni/Cu/Ag Plated Front Contact Single Crystalline Solar Cells. *IEEE J. Photovoltaics* **2016**, *6* (5), 1090–1093. https://doi.org/10.1109/JPHOTOV.2016.2576683.

(42) Colwell, J.; Hsiao, P.-C.; Shen, X.; Zhang, W.; Wang, X.; Lim, S.; Lennon, A. Impact of Contact Integrity during Thermal Stress Testing on Degradation Analysis of Copper-Plated Silicon Solar Cells. *Sol. Energy Mater. Sol. Cells* **2018**, *174*, 225–232. https://doi.org/10.1016/j.solmat.2017.09.005.

(43) Oikawa, H.; Takei, H.; Karashima, S. Interdiffusion in Copper-Rich Cu-Ag Solid Solutions. *Metall. Trans.* **1973**, *4* (3), 653–655. https://doi.org/10.1007/BF02643070.

(44) Subramanian, P. R.; Perepezko, J. H. The Ag-Cu (Silver-Copper) System. *J. Phase Equilibria* **1993**, *14* (1), 62–75. https://doi.org/10.1007/BF02652162.

(45) Witusiewicz, V. T.; Hecht, U.; Fries, S. G.; Rex, S. The Ag–Al–Cu System. *J. Alloys Compd.* **2004**, *385* (1–2), 133–143. https://doi.org/10.1016/j.jallcom.2004.04.126.

(46) Wang, C. P.; Yan, L. N.; Han, J. J.; Liu, X. J. Diffusion Mobilities in the Fcc Ag–Cu and Ag–Pd Alloys. *Calphad* **2012**, *37*, 57–64. https://doi.org/10.1016/j.calphad.2012.01.001.

(47) DiGiacomo, G.; Peressini, P.; Rutledge, R. Diffusion Coefficient and Electromigration Velocity of Copper in Thin Silver Films. *J. Appl. Phys.* **1974**, *45* (4), 1626–1629. https://doi.org/10.1063/1.1663466.

(48) Butrymowicz, D. B.; Manning, J. R.; Read, M. E. Diffusion in Copper and Copper Alloys, Part II. Copper-Silver and Copper-Gold Systems. *J. Phys. Chem. Ref. Data* **1974**, *3* (2), 527–602. https://doi.org/10.1063/1.3253145.

(49) Dorner, P.; Gust, W.; Hintz, M. B.; Lodding, A.; Odelius, H.; Predel, B. SIMS Investigations on the Diffusion of Cu in Ag Single Crystals. *Acta Metall.* **1980**, *28* (3), 291–300. https://doi.org/10.1016/0001-6160(80)90164-9.

(50) Lin, T. Y.; Pecht, M. G.; Das, D.; Pan, J.; Wenhui, Z. The Evaluation of Copper Migration during the Die Attach Curing and Second Wire Bonding Process. *IEEE Trans. Components Packag. Technol.* **2005**, *28* (2), 337–344. https://doi.org/10.1109/TCAPT.2005.848494.

(51) Li, W.-H.; Joelle Ong, S. W. Cu Diffusion in Ag-Plated Cu Leadframe Packages. *Microelectron. Reliab.* **2012**, *52* (7), 1523–1527. https://doi.org/10.1016/j.microrel.2012.02.022.

(52) Zhang, L.; Zhu, Y.; Wang, W.; Bi, X.; Chen, H.; Leung, K.; Wu, Y.; Wu, J. Study on Ag-Plated Cu Lead Frame and Its Effect to LED Performance Under Thermal Aging. *IEEE Trans. Device Mater. Reliab.* **2014**, *14* (4), 1022–1030. https://doi.org/10.1109/TDMR.2014.2360081.

(53) Marquis, E. A.; Chen, Y.; Kohanek, J.; Dong, Y.; Centeno, S. A. Exposing the Sub-Surface of Historical Daguerreotypes and the Effects of Sulfur-Induced Corrosion. *Corros. Sci.* **2015**, *94*, 438–444. https://doi.org/10.1016/j.corsci.2015.02.018.

(54) Grieten, E.; Schalm, O.; Tack, P.; Bauters, S.; Storme, P.; Gauquelin, N.; Caen, J.; Patelli, A.; Vincze, L.; Schryvers, D. Reclaiming the Image of Daguerreotypes: Characterization of the Corroded Surface before and after Atmospheric Plasma Treatment. *J. Cult. Herit.* **2017**, *28* (2017), 56–64. https://doi.org/10.1016/j.culher.2017.05.008.

(55) Peike, C.; Hoffmann, S.; Hülsmann, P.; Thaidigsmann, B.; Weiß, K. A.; Koehl, M.; Bentz, P. Origin of Damp-Heat Induced Cell Degradation. *Sol. Energy Mater. Sol. Cells* **2013**, *116*, 49–54. https://doi.org/10.1016/j.solmat.2013.03.022.

(56) Gawlinska-Necek, K.; Socha, R. P.; Balawender, P.; Stodolny, M. K.; Van Aken, B. B.; Starowicz, Z.; Panek, P. Silicon Solar Cells and Modules with Front Contact Paste Containing Copper-Based Component. *Prog. Photovoltaics Res. Appl.* **2021**, *29* (9), 1008–

1019. https://doi.org/10.1002/pip.3424.

Table of contents graphic: